Available online at www.sciencedirect.com
SCIENCE DIRECT®
International Journal of Multiphase Flow 31 (2005) 452–472
International Journal of Multiphase Flow
www.elsevier.com/locate/ijmulflow

A neutron scatterometer for void-fraction measurement in heated rod-bundle channels under CANDU LOCA conditions

J.R. Buell [a], D.P Byskal [a], M.R. Desrosiers [b], E.M.A. Hussein [b,*], P.J. Ingham [a], R.S. Swartz [a]

[a] *Experimental Thermalhydraulics and Combustion, AECL Whiteshell Laboratories, Pinawa, Manitoba, Canada R0E 1L0*

[b] *Department of Mechanical Engineering, University of New Brunswick, P.O. Box 4400, Fredericton, New Brunswick, Canada E3B 5A3*

Received 9 September 2004; received in revised form 15 December 2004

Abstract

The difficult problem of directly measuring the void fraction of rapidly boiling water in rod-bundle channels, such as those simulating a large loss-of-coolant accident (LOCA) in a nuclear reactor, is overcome by using a fast-neutron scattering device (scatterometer). The neutron scatterometer measures the number of neutrons scattered from a test section exposed to fast neutrons, and relates these measurements to the channel void fraction. The concept of the device and its design features are discussed. Such a scatterometer was constructed and installed on a test section (channel) of the RD-14M Thermalhydraulic Test Facility of Atomic Energy of Canada Limited. Experiments (30-mm diameter break in the inlet header) were conducted to evaluate the scatterometer's performance under transient conditions. Results of these tests show that the scatterometer can continuously measure the channel void fraction to within ±10% void (95% confidence interval) when corrections for non-linearity and time response are applied.

Keywords: Void fraction; Transients; LOCA; Neutron scattering

* Corresponding author. Tel.: +1 506 447 3105; fax: +1 506 453 5025.
E-mail address: hussein@unb.ca (E.M.A. Hussein).

0301-9322/$ - see front matter © 2005 Elsevier Ltd. All rights reserved.
doi:10.1016/j.ijmultiphaseflow.2005.01.004

1. Introduction

Void is the direct indicator of coolant starvation. Therefore, its measurement is essential for assessing reactor performance during postulated loss-of-coolant accident (LOCA) conditions, and for validating computer codes utilized in reactor safety analysis. Measuring void in rod-bundle geometries (simulating reactor fuel) during transients, such as critical or large break LOCAs, has proven to be very difficult, primarily due to the typically large ratio of metal-to-liquid volume in such channels. The metal of the rod bundles and surrounding vessels or channel walls masks the water content. This challenge faced workers who attempted to measure the void fraction in the rod-bundle geometries of boiling water and pressurized water reactors (BWRs and PWRs); and in the horizontal channels of CANDU[1] reactors. The typically high operating pressure and the intricate nature of the rod-bundle geometry make it difficult to introduce intrusive probes. Most reported techniques focused on the use of penetrating radiation (gamma rays or neutrons) to overcome the overwhelming presence of the metallic rods. When non-radiation techniques, such as capacitive void fraction sensors, were applied to rod-bundle geometry, they were used with plastic (Perspex) models (e.g., Kok et al., 1995).

When radiation methods are used for void-fraction measurement, the transmission method is usually applied, where the intensity of a transmitted radiation beam (or beams) is measured to provide a chordal void-fraction measurement along the path of radiation within the test object. The transmission method can be used in conventional gamma densitometry (e.g., Hori et al., 1996), for radiographic imaging (e.g., Takenaka et al., 1998), or in tomographic imaging (e.g., Kok et al., 2001). Tomographic imaging requires the collection of a large amount of measurements at different orientations, hence a relatively long total measurement time. However, the response of gamma-ray densitometry is dominated by the high density and high content of the metal in the rod bundle, which forced previous workers (Akiyama et al., 1995) to utilize a lower density metal (titanium alloy) in the void measuring section. The same workers also had to design a multibeam system, consisting of twelve narrow beams; the width of each was designed to avoid the interaction of gamma-rays with heater rods or walls. Even then, Akiyama et al. reported rod-bundle void measurements at steady-state conditions, and performed transient measurements only in test sections containing a quarter section of an actual heater rod. Our experience with a wide-beam gamma densitometer also confirmed that such a device could not meet the requirements of fast-transient measurements. Neutron radiography overcomes the shadowing effect of the metallic rods that overwhelms gamma-ray radiography. Even then, neutron radiography dictated the use of reactor beams (Takenaka et al., 1998) to provide the necessary high radiation intensity required for high quality radiography, and was only applicable under steady-state conditions.

Due to the above difficulties, fast neutrons were deemed more suitable for this measurement problem. Fast neutrons lose most of their energy upon colliding with the hydrogen nuclei, present in water. On the other hand, neutrons hardly lose any energy upon collision with the nuclei of a metal. Therefore, the slowing-down of fast neutrons is a natural way for distinguishing between water and metal. Such slowing-down is best measured by recording scattered neutrons. Scattering provides flexibility in locating the source and detector(s), which do not have to be on opposing sides of the test object as in conventional transmission techniques. Moreover, scattering avoids

[1] CANDU® (CANada Deuterium Uranium) is a registered trademark of Atomic Energy of Canada Limited (AECL).

the collimation process and precise alignment of the source with the detector, which is necessary in transmission measurements. Moreover, with scattering, more than one detector can be employed for the same source, which increases the overall registered count rate. The scattering modality also offers higher detection efficiency, owing to the lower energy of the slowed-down neutrons. Neutrons also encounter many collisions before reaching a scattering detector, thus they provide a form of spatial averaging and yield measurements that are less sensitive to the phase distribution. This spatial averaging process limits the use of the technique to bulk measurement of void fraction.

The scattering of fast neutrons was used for void-fraction measurement of two-phase flow by a number of workers; some relied on neutron beams extracted from a nuclear reactor (Rousseau et al., 1976; Banerjee et al., 1978, 1979; Deruaz and Freitas, 1983), while others employed radioisotopic sources (Frazzoli et al., 1978; Frazzoli and Magrini, 1979; Hussein and Waller, 1990; Waller and Hussein, 1990). The applications covered pipe inner diameters as small as 12 mm (Deruaz and Freitas, 1983), and as large as 112.8 mm (Hussein and Waller, 1990), with metallic pipe thickness as large as 10 mm (Frazzoli et al., 1978). Methods to design such scatterometers, for linearity and minimum dependence on flow-regime configuration, were suggested by Yuen et al. (1988) semi-empirically, and Hussein (1988) analytically. Both these methods aimed at optimizing the scatterometer for a linear response (for ease of calibration) and for flow-regime independence (to eliminate the need to know the spatial phase distribution). Banerjee et al. (1979) applied the technique to a rod bundle made of empty unheated zirconium tubes, and employed a neutron beam extracted from a nuclear reactor. Since zirconium is a weak neutron absorber, it is effectively transparent to neutrons, and served in the above mentioned work as a flow separator. It is worth noting that at least two patents have been issued in relation to this technique (Banerjee and Aggour, 1985 and Lim et al., 1990).

Given the above mentioned advantages of fast-neutron scattering, a neutron scatterometer was designed for measuring the void fraction in rod-bundle channels. The design, implementation and on-line testing of this device is discussed in this paper.

2. Test loop and requirements

The design of the void measurement device was tailored to measure void in the rod-bundle channel of the RD-14M Thermalhydraulic Test Facility at the Whiteshell Laboratories of Atomic Energy of Canada Limited, a schematic of which is shown in Fig. 1. This is an 11-MW full-elevation-scaled loop possessing most of the key components of the primary heat transport system for a CANDU reactor. The working liquid in RD-14M is light water, unlike heavy water which is found in CANDU reactors. The facility is arranged in the standard CANDU two-pass, figure-of-eight configuration. The reactor core is simulated by ten, 6-m-long horizontal channels (test sections). Each test section has simulated end-fittings and seven electrical heaters, or fuel element simulators (FES), designed to have many of the characteristics of the CANDU fuel bundle. A cross-section of a heated section is depicted in Fig. 2. Experiments are conducted in RD-14M to improve the understanding of the thermal-hydraulic behaviour of a CANDU reactor during loss-of-coolant accidents (LOCA), under forced and natural circulation conditions, and during shutdown scenarios. The data collected from this facility are used to identify and examine

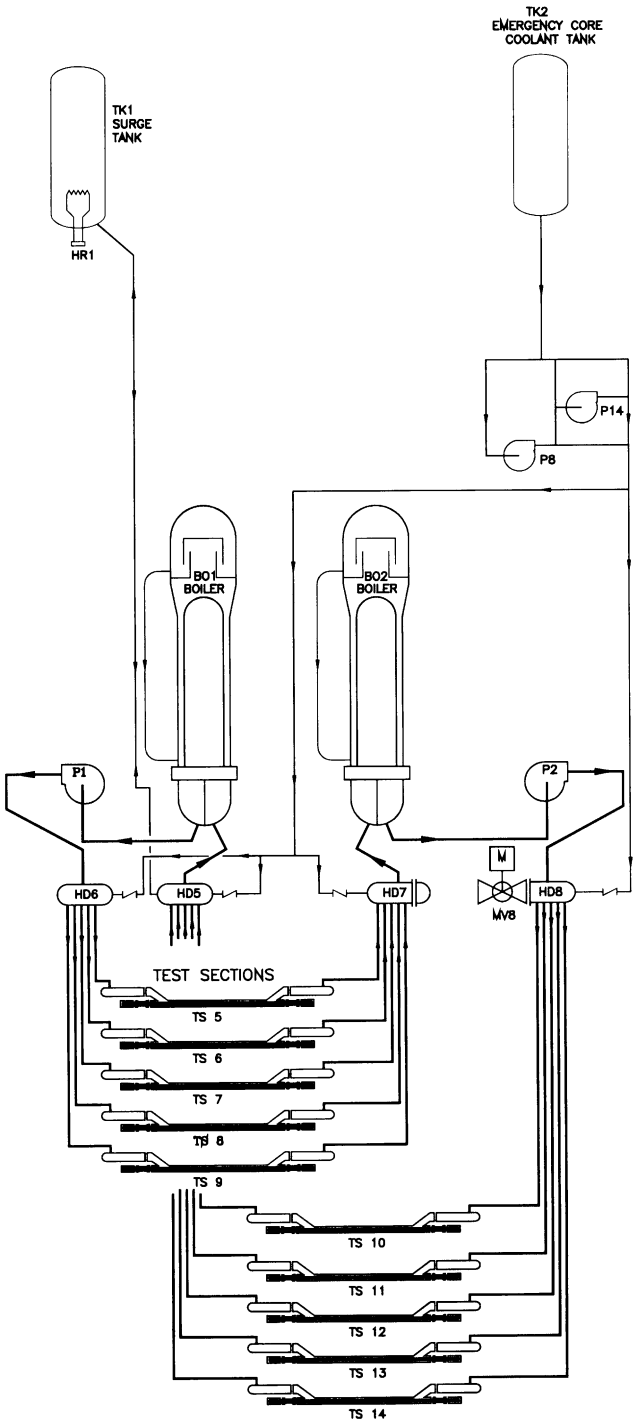

Fig. 1. RD-14M loop schematic.

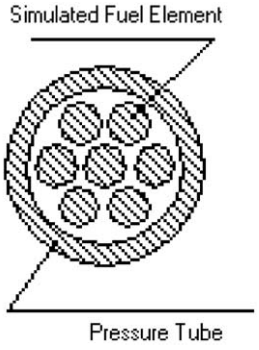

Fig. 2. Cross-section of heated section in RD-14M.

thermal-hydraulic phenomena and form a database for use in developing and validating computer models used to predict CANDU reactor behaviour. The code validation process requires an accurate channel void-fraction measurement during the overpower transient (power pulse) that can occur under some LOCA conditions, as a consequence of the positive reactivity-coefficient for void that exists in CANDU reactors. The coolant voiding rate determines the rate of positive reactivity insertion during a LOCA event and governs the magnitude of the resulting overpower transient. Thus an instrument capable of accurately measuring the channel void for these postulated scenarios is needed.

In order to meet the above measurement needs, while realizing the difficulty of this measurement problem, the following minimum specifications of void fraction were designated:

- No more that 10% uncertainty at 95% confidence level (2-σ around the mean, where σ is the standard deviation), and
- a sampling rate of 10 Hz (i.e., every 0.1 s) or better.

It was also decided to devote effort towards obtaining a cross-sectional average void-fraction measurement during the initial stage of instrumentation development.

3. Reconfiguration

The concept of neutron scatterometry relies on measuring the number of neutrons scattered after being slowed-down (thermalized) by the liquid (water) present in the test section. Therefore, the test section is exposed to a fast neutron source and a thermal-neutron detector is utilized to detect the neutrons that have slowed-down, and have scattered away from the direct path of the source particles. The detector count rate is then expected to linearly decrease as the void fraction increases, due to the diminished amount of liquid available for thermalizing the incident fast neutrons. Therefore, the void fraction is estimated using the relationship:

$$\hat{\alpha} = \frac{C(0) - C(\alpha)}{C(0) - C(1)} \tag{1}$$

where $\hat{\alpha}$ is the estimated void fraction, and $C(\alpha)$ is the scatterometer's response corresponding to an actual void fraction α. The above linear relationship is desirable for a number of reasons: (1) it provides a uniform void resolution, over the whole range of void fraction, (2) it results in a unique void fraction for every measured response; and (3) it enables easy calibration of the device by acquiring only two reference measurements, for an empty and full-of-water test section. Another desirable feature is to provide void-fraction measurements that are independent of the usually unknown flow-regime configuration. This feature can be best achieved by scatterometry, as opposed to through-transmission measurements. In scatterometry, the neutron encounters a number of collisions before reaching the detector, thus providing some form of averaging (mixing) over the entire section. The use of the average count rate of two or more detectors, which are located on opposite sides of the test section, further reduces the dependence of the estimated void fraction on the spatial distribution of the scattering medium (liquid phase).

Initial effort in scatterometer development focused on attaining the above two objectives of linearity and independence of flow-regime configuration. The initial design (Han et al., 1994, 1995), shown in Fig. 3, consisted of a fast neutron source (^{252}Cf) positioned at the side of the channel and two pairs of slow-neutron (^{3}He gas filled) detectors. The detectors were arranged such that one pair is located at the top of the channel and the other at its bottom. Cadmium sheets were used to surround the detectors and the shielding walls in order to minimize the number of background slow-neutrons within the detection cavity. The scatterometer was designed such that it had a linear response (for ease of calibration) and was not very sensitive to flow-regime variation. A more detailed explanation of the optimization of the source energy selection process is provided in Desrosiers and Hussein (1998). Monte Carlo simulations were also used to verify the linearity and flow-regime insensitivity of the technique in the rod-bundle geometry of the RD-14M test section; details of this study are given in Desrosiers (2000) and a summary is given in Hussein et al. (2000). These design criteria were also verified using bench-top experiments, and then the scatterometer was installed in the RD-14M loop in 1993 (Han et al., 1994 and Han, 1994). Its performance was assessed during a natural circulation test that lasted about nine hours, during which the scatterometer's counts were sampled every 12 s for a period of 10 s. The obtained results were

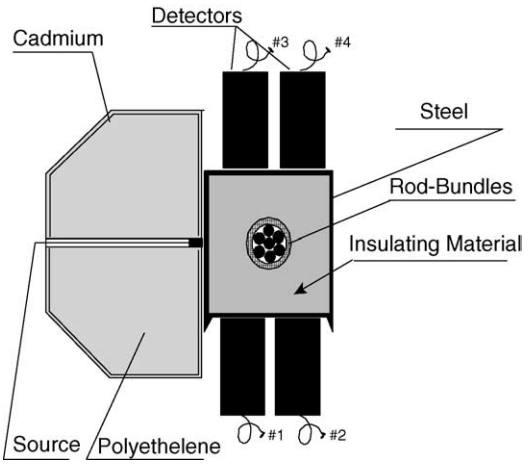

Fig. 3. Layout of initial scatterometer's design.

consistent with the void behaviour deduced from other independent measurements of flow, outlet fluid density, pressure, and temperature of fuel element simulators; see Han et al. (1994) and Han (1994). During these tests, the scatterometer had a one microgram ^{252}Cf source, emitting 2.3×10^6 neutrons/s. Over the counting period of 10 s (i.e., 0.1 Hz sampling rate), the scatterometer provided a maximum error in void fraction, $\Delta\alpha$, of about 11% (at a 2-σ, 95%, confidence level). Both the attained statistical accuracy and the sampling rate were well below the requirements for fast transients, stated in Section 2. The obvious solution to this problem is to increase the source strength to provide the required count rate for the desired uncertainty level within the designated counting period. The source activity must be strong enough not only to meet counting requirements but also to account for radioactive decay, due to the relatively short half-life of the source (2.645 years). Elevating the source activity also increases the biological shielding requirements, which can make the device quite bulky and cumbersome, and can hinder its implementation within the confined space of the RD-14M Facility. Therefore, attempts were made to optimize the performance of the device to obtain as high as possible contrast for a given source strength.

The contrast of the scatterometer is defined as

$$R = \frac{C(0)}{C(1)} - 1 \tag{2}$$

The effect of the contrast on the estimated value for α was shown (Desrosiers, 2000) to be governed by the relationship:

$$\Delta\alpha = \frac{1}{R\left(\sqrt{C_{\min}} - 1\right)} \tag{3}$$

where $\Delta\alpha$ is the uncertainty in α and $C_{\min}$ is the minimum obtainable count rate $= C(1)$. Eq. (3) indicates that $\Delta\alpha$ can be decreased by increasing the value of $C_{\min}$. The latter value can be directly elevated by (1) increasing the source strength, (2) prolonging the counting period, and/or (3) employing simultaneously many scattering detectors and using the sum of their count rates. The source strength cannot be increased indefinitely, and the source itself decays with time. The counting interval is limited to 0.1 s or less, given the mandated sampling rate of 10 Hz. Effort was therefore focused on finding ways to increase the value of R without requiring unrealistically high source strength.

As Eq. (3) indicates, by increasing the contrast ratio, R, the required minimum count rate can be decreased, for the same level of uncertainty in the void fraction, $\Delta\alpha$. Therefore, various factors affecting the contrast ratio were examined in an attempt to increase its value, from the 6% contrast ratio of the original design to as large as practically possible. To this end, a systematic parametric study was performed to determine the factors that have the strongest effect on the value of R.

Eq. (2) indicates that increasing the contrast requires decreasing the count rate for an empty channel, $C(1)$. This is equivalent to stating that the contrast of the scatterometer is increased if the background count rate is reduced, because neutrons do not slow-down in an empty channel. Then the detector would receive neutrons that reach it directly from the source, or after being scattered by the channel or the surrounding shielding material. The detectors were wrapped in cadmium, except for the surface facing the channel, so that only neutrons with energy above the cadmium cut-off energy (above 0.5 eV) could reach the detectors. Experimental testing of this

design showed that the sub-cadmium (below 0.5 eV) background neutrons did not reach the detectors, as the background count rate did not change when the detectors were fully wrapped with cadmium. Therefore, the background component was attributed to the epi-cadmium/fast (above 0.5 eV) neutrons. Monte Carlo simulations indicated that significant reduction of the background component was possible, leading to high contrast ratios.

A number of approaches were attempted to reduce the background component and enhance the contrast (Gallant, 1997 and Desrosiers, 2000). Some of the methods were not practical for on-line measurements, e.g., taking the difference between two measurements, and others were not very effective, such as changing source energy and detector location and/or type. However, it was found that aligning detectors with their axes parallel to that of the channel, was beneficial in two ways. First, it increased the contrast ratio from about 6% (with the original configuration where the detectors were perpendicular to the channel) to 9%. Second, the count rate also doubled, due to the increased field-of-view of the detector to scattered neutrons. In addition, it was found that bringing the source as close to the channel as practically possible was quite helpful. Originally, the source was butted against the thermal-insulation box surrounding the channel; designed to keep as much heat as possible within the channel, for maximum heat deposition in the coolant. Monte Carlo simulations showed that the contrast ratio, R, of the scatterometer can be increased up to about 36% by bringing the source as close as possible to the channel; instead of having it positioned outside the thermal-insulation box (Desrosiers, 2000). This increase in the contrast was attributed to the increase in the number of neutrons (per unit source) that were subjected to slowing-down by the liquid in the channel, and to the decrease of the background caused by the slow neutrons scattered by the hydrogen in the shielding of the device. The simulations also showed that the increase in the contrast ratio comes at the expense of reduced count rate. Therefore, the contrast ratio cannot be increased indefinitely while maintaining a high count-rate per unit source. Laboratory experiments performed with the source in contact with the channel showed that indeed the contrast ratio, R, increased, as the Monte Carlo simulation indicated. However, the value of R increased only to about 12.5%. (with the detector orientation changed as indicated above). All other attempts in the laboratory to increase the contrast ratio by reducing the background (i.e., the count rate for an empty channel) failed.

In a last-resort effort to reduce the background signal of fast neutrons, it was decided to remove the radiation shielding altogether. Neutrons scattered by the hydrogen in the shielding have a reduced energy, hence a higher probability of detection. Although removing the shielding is not practically possible, it was permitted in the laboratory by using a very weak source. This radical step led to an increase in the contrast ratio to close to 18%, three times the original value. Eliminating the shielding, as far as the detectors are concerned, is equivalent to moving the source and the shielding away from each other, as far as practically possible, so that the neutrons reflected off the shielding are spread over a large area. This in turn minimizes the portion of the reflected neutrons that reach the detector. Moving the shielding back by about 0.38 m was found to be almost equivalent to having no shielding at all, i.e., producing a contrast ratio of about 18%, while not drastically reducing the count rate.

Increasing the number of detectors, and using the summation of the response of individual detectors, directly reduces the required source strength by a factor of $1/N$, where N is the number of detectors. This a unique feature of scattering techniques, not offered by transmission-based methods.

In summary, the scatterometer contrast was enhanced significantly, without a highly elevated source activity, by (1) bringing the source as close as possible from the inspected channel, (2) moving the shielding at least 0.38 m from the channel, (3) orientating the detector parallel to it, and (4) increasing the number of detectors. With four detectors, it was estimated that the minimum source strength required to meet the specifications is 28.22 μg. Therefore, a 50 μg source will give an error in void fraction better than 10% (at 2-σ), until it decays to 28.42 μg, which will take about 0.815 half-lives or $0.815 \times 2.645 = 2.15$ years.

4. Design and construction

Based on that above considerations, a device was designed and constructed at the RD-14M Test Facility. The basic components of the device are described below.

4.1. Source

A ^{252}Cf neutron source initially with 2 GBq activity (100 μg) was acquired for the device. This source strength is higher than the recommended source activity to accommodate any unforeseen uncertainties in acquiring the data at high rate (10 Hz), and to ensure a longer lifetime of operation at the desired level of accuracy. The source is 5.5 mm in outside diameter and 11.94 mm in length, including the welded stainless steel container. The source was housed in either one of two separate shielding systems. The neutron source is normally stored at the centre of a storage container. The storage container has a shutter that can be raised so that the neutron source can be deployed from the storage container. When the scatterometer is used for experimental measurements, the source is deployed to the target (at a particular axial location on an RD-14M heated section). The experimental shielding box provides radiological shielding when the source is deployed. A push rod is used to move the source between the shielding container and the experimental shielding box.

When deployed at the target, the source is situated against the side of the RD-14M heated-section pressure tube. A hole in the side of the heated-section strongback allows the source to be deployed directly to the pressure tube, as shown in Fig. 4.

An essential part of the design is that the inside-walls of the shielding box are a minimum of 430 mm from the source. This design minimizes the sensitivity to thermal neutrons backscattered from the experimental shielding box.

The principle of as low as reasonably achievable (ALARA) was applied to the shielding design of the scatterometer. Due to physical constraints in the RD-14M loop, the scatterometer could only be fabricated to a limited size. The shielding design, given the space limits, reduced dose rates to the same levels as those of existing RD-14M gamma densitometers.

4.2. Detectors

The scatterometer has eight neutron detectors as shown in Fig. 4, used to measure the scattered neutrons. This was double that used to determine the required source strength to further increase the scatterometer's overall count rate. The eight ^{3}He gas (10 MPa) detectors, 50 mm in diameter

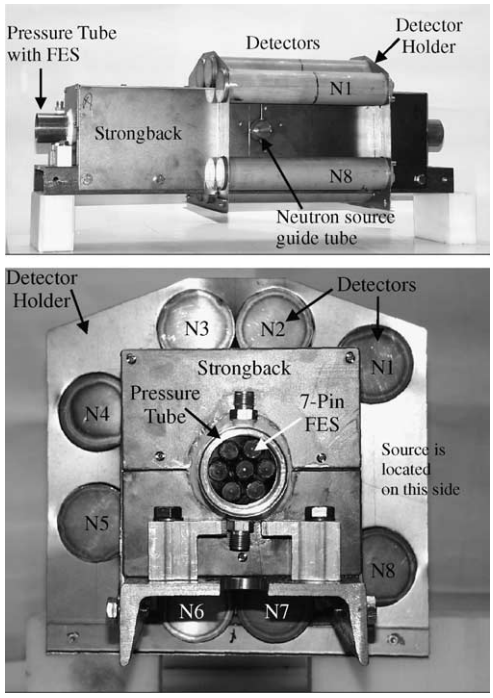

Fig. 4. A picture of the scatterometer, showing source and detector locations around a simulated test section.

and 165 mm long operated in current mode. The current outputs of the detectors are amplified, time averaged, and converted to voltages that can be sampled by the RD-14M data-acquisition system. Thus, the scatterometer output voltages vary with changes in the heated-channel void fraction. Each detector is cylindrical, and was set-up with its axis in the same direction as to that of the heated-section pressure tube, i.e., the cylinders of the detectors and the tube are parallel to each other. The axial centre of each detector is aligned, as close as possible, with the centre of the neutron source when the source is deployed at the heated-section pressure tube.

The actual detector is housed within a cylindrical tube. The cylindrical tube electrically isolates the detector. This is necessary because the bias voltage is applied to the outside casing of the detector. A pre-amplifier is contained within one end of the cylindrical tube.

4.3. Scatterometer location

The neutron scatterometer was installed at one of the heated sections of the RD-14M loop, Heated-section 14 (HS14). The scatterometer (when deployed) was centred 4.740 m from the inlet end of the heated section (that is, from the start of the heated FES portion). This corresponds to segment number ten (10) of the twelve (12) segments of the heated section, with segment one (1) being closest to the inlet of the channel. The total heated length is 6 m.

Because the detectors are finite in length and the neutron source radiates in all directions, the neutron scatterometer will be influenced by changes in void fraction over a certain length of the channel. Zone-of-influence tests were performed to determine this length, with the simulated test

section installed in a vertical orientation. The channel was initially empty, then water at room temperature and pressure was added gradually to specific levels, and data were recorded. A level was inferred from a differential pressure measurement. The results showed a zone-of-influence of approximately 250 mm (125 mm along the channel, on each side of the source). The response within the zone-of-influence was highly non-linear, with over 91% of the sensitivity in the ±150-mm range. The neutron scatterometer does not respond to void fraction changes outside the zone-of-influence. It should be kept in mind that the results obtained are spatially averaged over the zone-of-influence, which is equivalent to about half the length of one of the 12 bundles in each channel. This spatial resolution is sufficient for this work.

5. Calculation of void fraction

This section describes the process used to calculate the void fraction from recorded measurements. First the void fraction is calculated assuming a linear response. The value is then corrected to take into account the time response for the device. Finally, non-linear variations in the response are accounted for.

5.1. From linear response

The outputs of the scatterometer are voltage signals for each detector channel. Assuming a linear scatterometer response, the void fraction for each of the eight detectors is calculated as

$$\alpha'_i = \frac{V_i - V_{\mathrm{f},i}}{V_{\mathrm{e},i} - V_{\mathrm{f},i}} \tag{4}$$

where α'_i is void fraction estimated from the voltage output V_i, of the detector i, and $V_{\mathrm{f},i}$ and $V_{\mathrm{e},i}$ are, respectively, the voltage outputs of the same when the channel is full (liquid filled) and empty (vapour filled). While $V_{\mathrm{f},i}$ and $V_{\mathrm{e},i}$ are reference voltages, V_i, is a function of time. However, the output of the scatterometer will vary with changes in the liquid density, which is particularly important during RD-14M LOCA experiments. This means that $V_{\mathrm{f},i}$ in Eq. (4) will shift in value as the liquid density changes. Fortunately, however, this shift was found to be linear and was determined from a simple heat-up experiment in RD-14M. For each detector, the correction for the shift in the full reading is given by

$$V_{\mathrm{f},i} = V_{\mathrm{f0},i} + \beta_i \cdot \left(\rho_f - \rho_{\mathrm{f0}}\right) \tag{5}$$

where $V_{\mathrm{f0},i}$ is the calibration reading (full channel) for detector i, β_i is a linear correction factor for detector i, ρ_{f0} is the channel liquid density when the calibration reading was taken, and ρ_{f} is the channel liquid density (as a function of time determined from pressure and temperature measurements). The recorded full readings ($V_{\mathrm{f0},i}$ for each detector channel) are taken under single-phase liquid conditions. For an RD-14M LOCA experiment, the full readings are taken just prior to the initiation of the blowdown, and the empty readings ($V_{\mathrm{e},i}$) are taken at the end of the experiment when the channel is filled with superheated steam.

The global void fraction is calculated as the average of the inferred void fractions for each detector channel:

$$\alpha' = \frac{\sum_{i=1}^{8} \alpha'_i}{8} \tag{6}$$

This void fraction is cross-sectional averaged, since all detectors are approximately uniformly distributed around the pressure tube. It is also volume-averaged, since the detector response is affected by changes in void fraction anywhere along the axial zone-of-influence.

5.2. Correction for time response

Since transients can occur very rapidly, it is important to quantify the time response within which the scatterometer (taking into account the detectors, pre-amplifier, and amplifier), will respond to a step change. This response was measured in a simulated RD-14M test section, by dropping a cylindrical polyethylene block through a vertical extension pipe connected to the scatterometer, and observing the scatterometer's response. The test piece consisted of a cylindrical polyethylene block machined to loosely fit within the extension pipe. The polyethylene block had several longitudinal holes through which FES rods were placed such that the cross-section was the same along the entire length. The length of the test piece was longer than the scatterometer zone-of-influence. A lead block was used to rapidly decelerate the test piece. Once stopped, the test piece completely spanned the scatterometer's zone-of-influence. Thus, the drop tests simulated a rapid change in void fraction. Three fast response (0.5 ms) infrared sensors were installed to detect the presence/absence of the test piece. Thirteen drop tests were carried out and their average was used to get an overall average response as a function of time.

The system was modelled as two first-order systems in series: one represents the detectors/pre-amplifier, and the other representing the amplifier, with τ_d and τ_a being the time constants of the first and the second circuits, respectively. Overall, this is equivalent to a second-order system:

$$\alpha'_\tau = \tau_d \tau_a \frac{d^2\alpha'}{dt^2} + (\tau_d + \tau_a)\frac{d\alpha'}{dt} + \alpha' \tag{7}$$

where α' is the linear estimate of the void fraction, τ_d is a first-order time constant of detectors/pre-amplifiers, τ_a is a first-order time constant of amplifiers, and α'_τ is the void fraction corrected for scatterometer time response. The channel void fraction (driving function), α'_τ, was determined from the response of the scatterometer versus distance from the source, and the velocity of the test piece. The time response of the neutron scatterometer amplifiers was determined by introducing a square wave to the amplifier as an input and recording the output. The time constant of the detector/pre-amplifier system, τ_d, is the only unknown in Eq. (7), and was solved for numerically, yielding a value of τ_d.

Based on the above model, it was estimated that it takes approximately 0.135 s for the neutron scatterometer to reach 95% response to an instantaneous change in void. The two derivative terms in Eq. (7) were estimated using a central-difference scheme applied to the measured void fraction, α'.

5.3. Calibration (correction for non-linearity)

The relationship between the scatterometer outputs and the actual channel void fraction was obtained by examining the behaviour under various void fractions and flow regimes. In order

to perform controlled, steady-state tests at different void fractions and flow regimes, polyethylene was chosen to mimic liquid water. Polyethylene and water have similar hydrogen content, and the neutrons are slowed-down by the hydrogen to give different detector outputs at different void fractions. Polyethylene is also easily machinable, and spool pieces were made to simulate different void fractions and different flow regimes.

Homogeneous, annular, and stratified flow-regimes were simulated over a range of void fractions between 0.15 and 0.88. These results indicated a slightly non-linear behaviour that resulted in a bias error of up to 0.08 in the calculated void fraction. Therefore, a correction was derived to minimize this error. The correction was obtained using a non-linear regression analysis routine, as a modified rational function that forces the functional fit through voids of 0.0 and 1.0. The corrected void fraction is given by a polynomial with a forced fit through voids of 0.0 and 1.0:

$$\alpha = 0.930\alpha'_\tau - 0.475\alpha'^2_\tau + 0.545\alpha'^3_\tau \tag{8}$$

where α'_τ is the void fraction corrected for time response. The resulting void fraction is a better estimate of the channel void fraction, with a reduced uncertainty due to non-linearity introduced by variation in phase distribution.

6. Performance under LOCA conditions

A number of on-line tests were performed on the RD-14M loop to evaluate the performance of the neutron scatterometer under LOCA conditions. Two of these tests are discussed here: tests C0102 and B0101, which were performed in March 2001. Test B0101 is a counterpart to commissioning test C0102. Each test had a 30-mm diameter break in the inlet header (HD8—see Fig. 1), with a channel-power ramp to reactor-typical decay-heat levels (from full-power conditions), and primary-pump exponential rampdowns (power and pump rampdowns were started 2 s following the break). No emergency-coolant injection was added to the loop, and each test was terminated following an extended period at decay-power levels. The average initial conditions are provided in Table 1, and the sequence of events is listed in Tables 2 and 3. These types of tests are characterized by an initial balance between the pumping forces and the forces associated with fluid exiting the break. This causes an initial flow split in the heated sections which sees fluid exiting the heated section from either end. This flow split reduces the fluid inventory in the heated section and results in rapid voiding and heat-up in the heated section. Maintaining the balance between the pump and break forces does not occur for an extended period of time and as the pump head degrades the break forces dominate and flow is re-established through the heated sections, albeit in a reverse direction.

The outputs of the scatterometer's eight detectors were sampled at a rate of 20 Hz, the fastest possible sampling rate for the RD-14M data-acquisition system. Full readings (liquid filled) for each detector channel were taken as an average of the data just prior to the blowdown of each test. Empty readings (vapour filled) for each detector channel were taken as an average of the data near the end of each test. At this stage of each test, the heated section was completely steam filled (superheated) as indicated by other measurements; namely temperature and inlet and outlet void measurements (using gamma densitometers).

Prior to the blowdown, the liquid in the channel is subcooled (based on temperature measurements), and the band of "noise" is the random uncertainty in the scatterometer (see Section 7 for

Table 1
Summary of initial conditions and set-up for tests C0102 and B0101

	Test C0102	Test B0101
Primary-side pressure	10.0 MPa(g)	10.0 MPa(g)
Secondary-side pressure	4.44 MPa(g)	4.52 MPa(g)
Primary-pump 1 speed	3574 rpm (100%)	3576 rpm (100%)
Primary-pump 2 speed	3603 rpm (100%)	3599 rpm (100%)
Heated-section 5 power	747 kW	747 kW
Heated-section 6 power	752 kW	753 kW
Heated-section 7 power	840 kW	852 kW
Heated-section 8 power	1007 kW	1018 kW
Heated-section 9 power	755 kW	762 kW
Heated-section 10 power	660 kW	658 kW
Heated-section 11 power	778 kW	781 kW
Heated-section 12 power	925 kW	925 kW
Heated-section 13 power	1105 kW	1095 kW
Heated-section 14 power	778 kW	778 kW
Boiler 1 level	58%	55%
Boiler 2 level	58%	55%
FES temperature trips	600 °C	600 °C
Break orifice	30-mm diameter at header 8	30-mm diameter at header 8
Break valve	Nominal 150-mm valve	Nominal 150-mm valve
Capacitors in the scatterometer RC integration circuits	0.82 μF	1.5 μF

Table 2
Procedure/significant events during test C0102

Time (s)	Event
0.0	Data collection started
10.0	Signal sent to break valve to open
12.0	Start of primary-pump rundown and power rampdowns
23.7	Surge tank manually isolated (header 7 pressure below 5.5 MPa(g))
154.95	Power supply 2 tripped resulting in loss of power to HS7 and HS8
330.44	Data collection stopped

Table 3
Procedure/significant events during test B0101

Time (s)	Event
0.0	Data collection started
30.0	Signal sent to break valve (MV8) to open
32.0	Start of primary-pump rundown and power rampdowns
42.7	Surge tank manually isolated (header 7 pressure below 5.5 MPa(g))
157.76	Power supply 2 tripped resulting in loss of power to HS7 and HS8
301.19	Data collection stopped

the uncertainty analysis). Similarly, approximately 60 s after the blowdown, the channel is superheated (again based on temperature measurements), and the band of "noise" is the random uncertainty in the scatterometer.

The channel void fraction, calculated using Eqs. (6)–(8), is plotted in Fig. 5 for B0101. The top graph shows the calculated channel void fraction for the entire test duration. The bottom graph

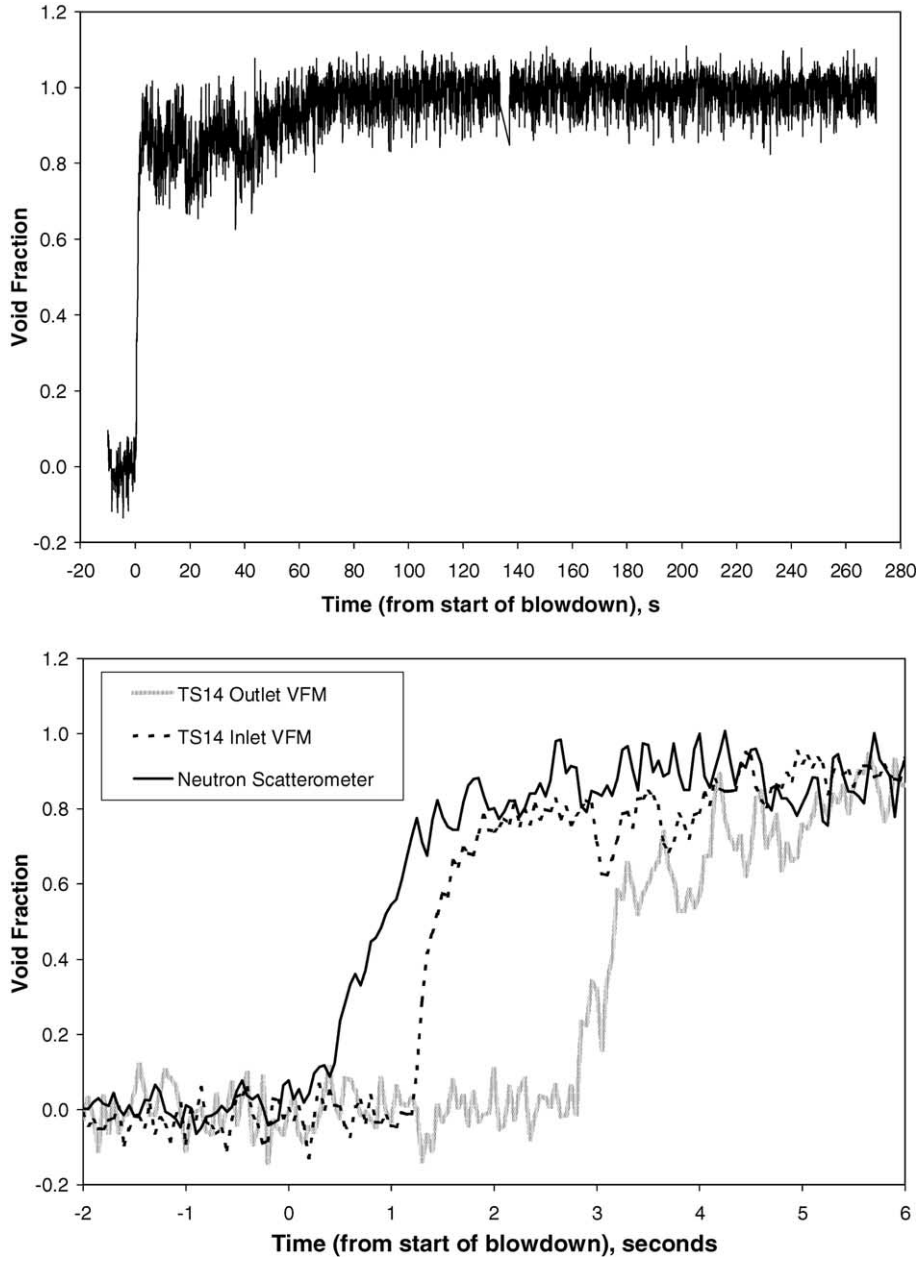

Fig. 5. Void fraction from neutron scatterometer and gamma densitometers (VFM), test B0101.

shows the calculated channel void fraction over the initial blowdown phase. This graph also shows the void fractions calculated from the inlet and outlet gamma densitometers. These densitometers are located on the inlet and outlet feeders near the end-fittings. The calculated channel

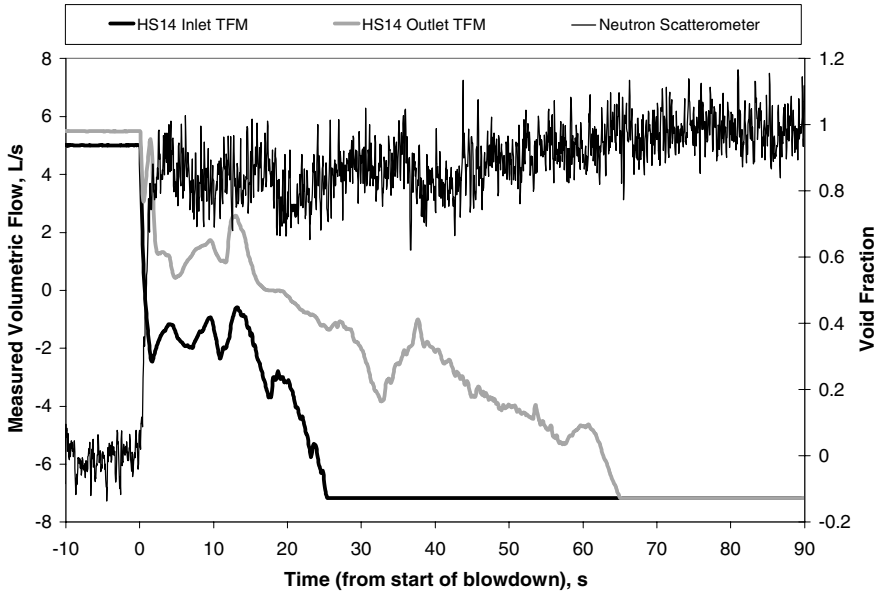

Fig. 6. Heated section (HS14) inlet and outlet flows from turbine flowmeters, test B0101.

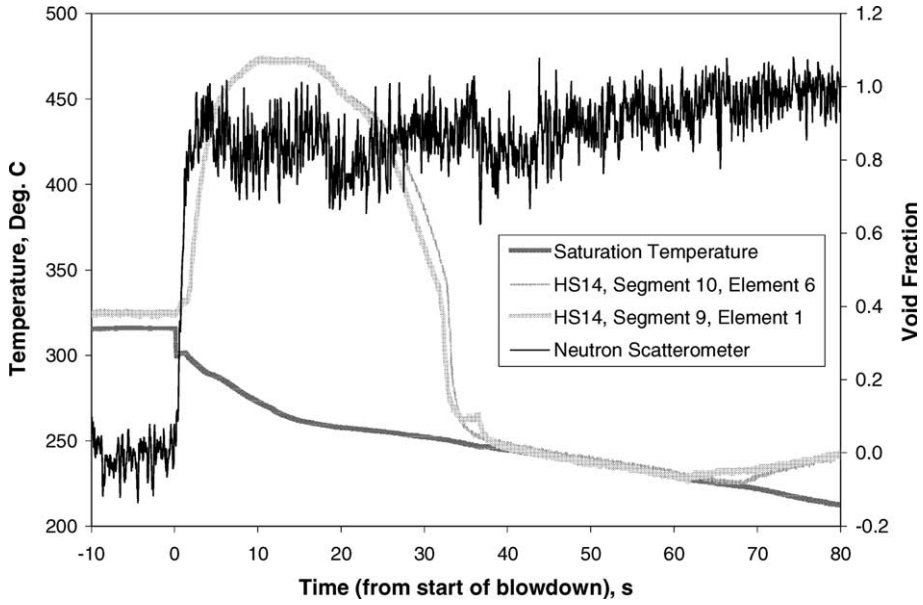

Fig. 7. Heated section (HS14) fuel element simulator (FES) temperatures, test B0101.

void fraction was consistent with the feeder void fractions (for this test, the flow initially exited both ends of the channel following the break—see Fig. 6).

The heated section (HS14) measured flow rates (using turbine flowmeters) and fuel element simulators (FES) temperatures for B0101 are shown in Figs. 6 and 7, respectively. Fig. 6 shows that a flow split developed in HS14 at approximately 1 s (the inlet flow reverses direction, i.e., becomes negative, while the outlet flow remains positive), and remained until approximately 16 s (outlet

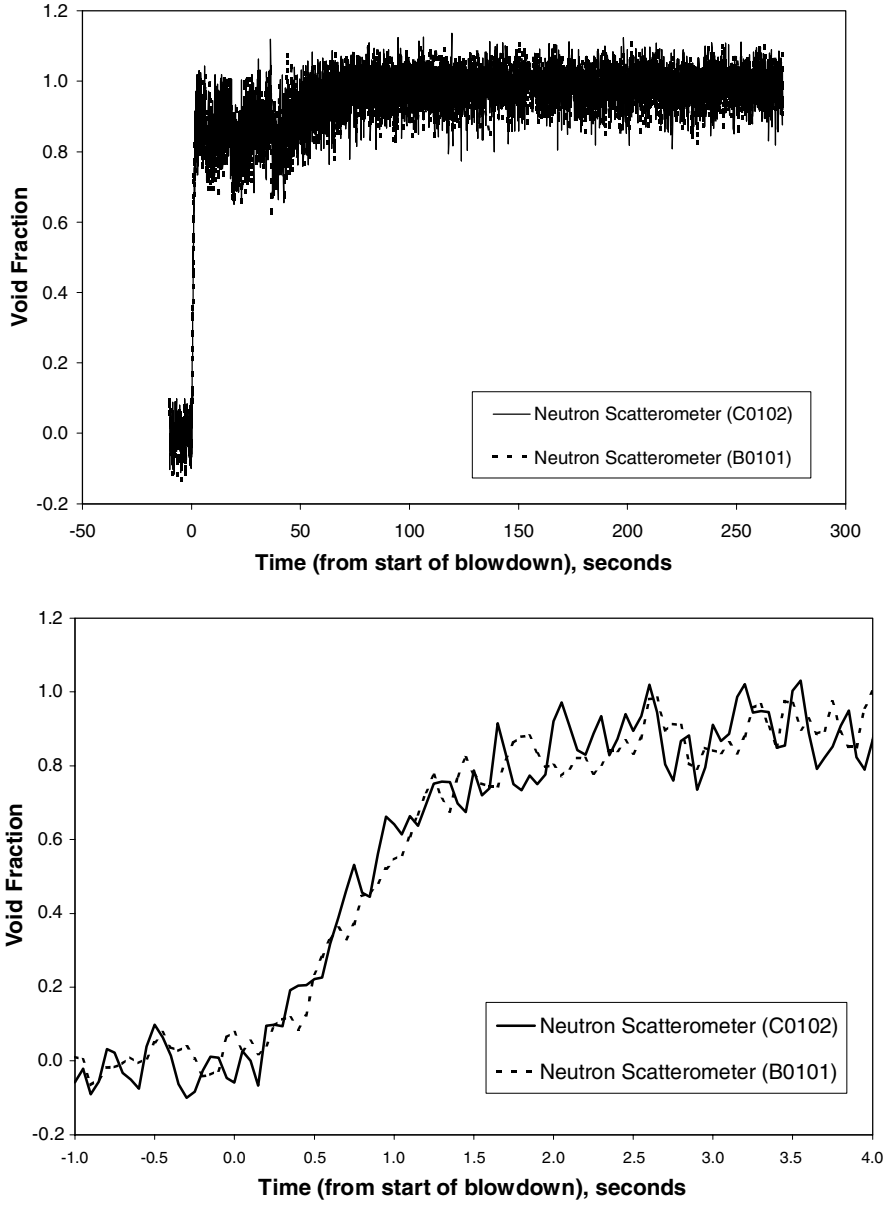

Fig. 8. Void fraction from neutron scatterometer, tests B0101 and C0102.

flow reversal occurs, leading to a total reversal of flow direction). After approximately 3 s, the flow through each turbine flowmeter was two phase, and eventually became single-phase steam. Peak HS14 FES temperatures (up to 477 °C) occurred between 10 and 18 s, and were followed by cooling to the saturation temperature (FES power was ramped down 2 s following the break). During this period, the calculated channel void fraction remained between 0.8 and 1.0. Heated-section 14 became superheated at approximately 70 s. At this point, the calculated channel void fraction indicated the channel was completely voided (empty). Fig. 8 overlays the measured channel void fraction from the two tests, C0102 and B0101, showing very good reproducibility.

7. Uncertainty analysis

The ANSI standard ANSI/NCSL Z540-2-1997 for instrument uncertainty analysis was used. This standard provides a methodology for identifying error types (random or systematic), and then combining these errors into an overall uncertainty. Dieck (1997) documented and discussed this standard.

The void fraction is calculated using Eqs. (6)–(8). Uncertainties in the input parameters to these equations were addressed. The voltage output from a detector channel as a function of time, V_i, has experimental uncertainty due to random error only, introduced by fluctuation in source emission and in the detection of neutrons. The random error in V_i is characterized by a standard deviation, which is calculated directly from the measured detector readings. For the same reasons, the full (liquid filled), $V_{f,i}$, and empty (vapour filled), $V_{e,i}$, readings have random errors. The empty reading was taken as an average reading over a period of time, and the random errors in $V_{f,i}$ and $V_{e,i}$ were characterized by the standard deviation of their average readings. In addition, uncertainty in the full reading, $V_{f,i}$, also depends on uncertainty of the liquid density correction, given by Eq. (5).

Systematic error may occur because of drift in $V_{f,i}$ and $V_{e,i}$. A long-duration stability test (RD-14M test C0101) was performed to determine the drift in the output signals of the detectors. Results of the stability test showed insignificant drift in the detector outputs with time, when compared with the uncertainties introduced from other error sources. Thus, systematic errors in the full and empty readings, due to signal drift, were ignored.

Eq. (8) is used to correct for non-linearity of the scatterometer response. However, even with the correction, a residual error remains. The residual error, referred to as the non-linearity bias error, is calculated from the scatter of the flow-regime calibration data. The non-linearity bias error was calculated to be ± 0.043 void.

The above random and systematic uncertainties were combined to give the overall random and systematic uncertainties in the global void fraction. The overall random and systematic uncertainties were then combined to give the overall void fraction uncertainty at the 95% confidence interval.

The overall uncertainties in the channel void fraction was ± 0.10 for both tests. This overall uncertainty was almost completely due to random fluctuations in the detector outputs (that is, random fluctuations in the voltages V_i), and systematic uncertainty due to non-linear behaviour. Systematic error, due to uncertainties in the empty and full readings, was negligible. This included any uncertainties introduced by the full-reading density correction, given by Eq. (5). The random fluctuations were reduced in test B0101, compared to C0102, by increasing the capacitance in the RC integration circuits of the scatterometer amplifiers.

Tests were also carried out to examine the random scatter in the neutron scatterometer output during a transient, with the purpose of showing that the uncertainty determined under steady-state conditions is valid under transient conditions. "Void insertion" tests were carried out by simulating channel voiding by removing polyethylene pieces at a fixed, controlled rate. These tests showed that the overall neutron scatterometer uncertainty of ± 0.1 void is applicable under transient voiding conditions.

8. Conclusions

A neutron scatterometer was designed, constructed, and installed on test section 14 of RD-14M. This scatterometer has eight neutron detectors operating in current mode. Procedures were developed for converting the detector signals into a cross-sectional average channel void fraction. Two RD-14M critical-break LOCA experiments (30-mm diameter break in the inlet header) were performed to evaluate the scatterometer performance under rapid transient conditions. Results of these tests show the scatterometer can measure the channel void fraction to within ± 0.1 void (95% confidence interval) at a rate of 10 Hz. Thus, the scatterometer has achieved all performance specifications.

A detailed analysis of the scatterometer time response was undertaken. The overall time response was modelled as two first-order systems in series: one representing the detectors/pre-amplifier, and the other representing the amplifier. The effect of the finite time response was to delay the indication of channel voiding, thereby causing a bias error in the calculated void fraction.

Uncertainty analysis showed that the most significant sources of uncertainty were the random fluctuations in the detector outputs and systematic uncertainty due to non-linear behaviour. The random fluctuations were reduced by increasing the capacitance in the scatterometer amplifier, slowing the time response. However, the scatterometer still easily captured the change in void fraction in the critical-break LOCA tests. This scatterometer is currently used to measure the channel void fraction in tests simulating various LOCA conditions.

This work enabled for the first time the application of the fast scattering technique to fairly rapid transients using a modest source activity and with a reasonable level of uncertainty. This was made possible by judicious utilization of the source neutrons by bringing the source as close as possible to the test object, removing the shielding to as far as practically possible from the source and the object, employing as many detectors as the space permitted and recording the counts in the current mode. Although this technique was specifically applied to a particular problem, it is equally applicable to any rapidly developing transients of low atomic number fluids contained within high atomic number structural materials. Such situations are encountered in chemical and power plants employing hydrogen-rich boiling or condensation fluids, in devices such as flow separators, heat exchangers, condensers and pressure vessels.

Acknowledgements

This work was funded by the CANDU Owners Group. The corresponding author acknowledges the fruitful discussion with members of the Co-ordinated Research Program on Bulk

Hydrogen Analysis using Neutrons, International Atomic Energy Agency. The work of the RD-14M technical staff in designing and constructing the RD-14M neutron scatterometer, and performing experiments to evaluate and develop the design, is also acknowledged. In particular, the efforts of the RD-14M loop supervisor, John Findlay, in suggesting and developing the current-mode electronics is acknowledged.

References

Akiyama, Y., Hori, K., Miyazaki, K., Mishima, K., Sugiyama, S., 1995. Pressurized water reactor fuel assembly subchannel void fraction measurement. Nucl. Technol. 112, 412–421.

Banerjee, S., Aggour, M., 1985. Apparatus and a Substance, U.S. Patent, #4,499,380.

Banerjee, S., Chan, A.M.C., Ramanathan, N., Yuen, P., 1978. Fast neutron scattering and attenuation techniques for measurement of void fractions and phase distribution in transient flow boiling. In: Sixth International Heat Transfer Conference, Toronto, 1978, vol. 1. Hemisphere Press, Washington, DC, pp. 351–355.

Banerjee, S., Yuen, P., Vandenbroke, M.A., 1979. Calibration of a fast neutron technique for technique void fraction in rod bundles. J. Heat Transfer Trans. 101, 295–299.

Deruaz, R., Freitas, R.L., 1983. Void fraction and pressure drop measurement in reflooded single tube. In: Plesset, M.S., Zuber, N., Catton, I. (Eds.), Transient Two-Phase Flow. Hemisphere, Washington, DC, pp. 227–242.

Desrosiers, M.R., 2000. Performance Enhancement of a Neutron scatterometer for Void Fraction Measurement. M.Sc.E. Thesis, University of New Brunswick, Fredericton, Canada.

Desrosiers, M.R., Hussein, E.M.A., 1998. Reducing fast-neutron sensitivity of slow-neutron detectors for use in neutron scatterometery. Report to the Research Program: Bulk Hydrogen Analysis, Using Neutrons. International Atomic Energy Agency, Vienna, Austria, November.

Dieck, R.H., 1997. Measurement Uncertainty Methods and Applications. Instrument Society of America, Research Triangle Park, NC.

Frazzoli, F.V., Magrini, A., 1979. Neutron gauge for measurement of high void fraction in water–steam mixture. Nucl. Technol. 45, 177–182.

Frazzoli, F.V., Magrini, A., Mancinic, C., 1978. Void fraction measurement of water–steam mixture by means of a californium-252 source. J. Appl. Isot. 29, 311–314.

Gallant, G., 1997. Reduction of Background Radiation in Neutron Scatterometery. M.Sc.E. Thesis. University of New Brunswick, Fredericton, Canada.

Han, P., 1994. Neutron scatterometer for Void-Fraction Measurement of Two-Phase Flow in Channels with Metallic Inclusions. Ph.D. Thesis. University of New Brunswick, Fredericton, Canada.

Han, P., Hussein, E.M.A., Ingham, P.J., Henschell, R.M., 1994. Nonintrusive measurement of transient flow boiling in rod-bundle channels using fast-neutron scattering. Nucl. Instrum. Methods Phys. Res. A353, 695–698.

Han, P., Hussein, E.M.A., Ingham, P.J., 1995. A neutron scattering device for void fraction measurement in channels of the RD-14M thermalhydraulics test facility. In: Proc. Canadian Nuclear Society Annular Conference, Saskatoon, Saskatchewan, vol. I, Section 2.2, pp. 12.

Hori, K., Miyazaki, K., Akiyama, Y., Nishioka, H., Takeda, N., 1996. Total evaluation of in bundle void fraction measurement test of PWR fuel assembly. In: Proc. ASME/JSME Int. Conf. on Nuclear Engineering, ICONE, vol. 1, n. Pt. 1B, New Orleans, LA, pp. 801–812.

Hussein, E.M.A., 1988. Modelling and design of a neutron scatterometer for void-fraction measurement. Nucl. Eng. Des. 105, 333–348.

Hussein, E.M.A., Desrosiers, M.R., Ingham, P.J., 2000. Two phase flow measurements with ^{252}Cf: design aspects and considerations. Trans. Am. Nucl. Soc. 82, 94–95.

Hussein, E.M.A., Waller, E.J., 1990. A neutron steam quality meter for a fluidized bed plant. Int. J. Radiat. Appl. Instrum.: Appl. Radiat. Isot. 41, 1049–1055.

Kok, H.V., Heerens, W.C., van der Hagen, T.H.J.J., van Dam, H., 1995. New principle for designing optimal capacitive void fraction sensors applied to a rod-bundle geometry. Meas.: J. Int. Meas. Confederation 15, 119–131.

Kok, H.V., van der Hagen, T.H.J.J., Mudde, R.F., 2001. Subchannel void-fraction measurements in a 6×6 rod bundle using a simple gamma-transmission method. Int. J. Multiphase Flow 27, 147–170.

Lim, G.B., Nieman, R.B., Banerjee, S., 1990. Method and Apparatus for Monitoring a Flowstream, U.S. Patent #4,924,099.

Rousseau, J.C., Czerny, J., Riegel, B., 1976. Void fraction measurement during blowdown by neutron absorption and scattering methods. OECD/NEA Specialists Meeting on Transient Two-Phase Flow, Toronto, Ont.

Takenaka, N., Asano, H., Fujii, T., Matsubayashi, M., 1998. Three-dimensional visualization of void fraction distribution in steady two-phase flow by thermal neutron radiography. Nucl. Eng. Des. 184, 203–212.

Waller, E.J., Hussein, E.M.A., 1990. A portable device for void fraction measurement in a small-diameter pipe. Nucl. Instrum. Methods A299, 670–673.

Yuen, P.S.L., Meneley, D.A., Banerjee, S., 1988. Measurement of void fraction by a neutron scattering technique with a portable source: effect of the incident energy spectrum. Int. J. Multiphase Flow 14, 401–412.